

UPDATED VERSION, August 23, 2018
 hep-ph/9507418
 CRN 95-26
 TK 95 16

THE REACTION $\pi N \rightarrow \pi\pi N$ AT THRESHOLD IN CHIRAL PERTURBATION THEORY

V. Bernard^{†,1}, N. Kaiser^{§,2}, Ulf-G. Meißner^{‡,3}

[†]Physique Théorique, Centre de Recherches Nucléaires
 B.P. 20, F-67037 Strasbourg Cedex 2, France

Université Louis Pasteur de Strasbourg, Institut de Physique,
 3-5 rue de l'Université, F-67084 Strasbourg, France

[§]Technische Universität München, Physik Department T39,
 James-Franck-Straße, D-85747 Garching, Germany

[‡]Universität Bonn, Institut für Theoretische Kernphysik,
 Nussallee 14-16, D-53115 Bonn, Germany

email: ¹bernard@crnhp4.in2p3.fr, ²nkaiser@physik.tu-muenchen.de,
³meissner@pythia.itkp.uni-bonn.de

ABSTRACT:

In the framework of heavy baryon chiral perturbation theory, we give the chiral expansion for the $\pi N \rightarrow \pi\pi N$ threshold amplitudes D_1 and D_2 to quadratic order in the pion mass. The theoretical results agree within one standard deviation with the empirical values. We also derive a relation between the two threshold amplitudes of the reaction $\pi N \rightarrow \pi\pi N$ and the $\pi\pi$ S-wave scattering lengths, a_0^0 and a_0^2 , respectively, to order $\mathcal{O}(M_\pi^2)$. We show that there are uncertainties mostly related to resonance excitation which make an accurate determination of the $\pi\pi$ scattering length a_0^0 from the $\pi\pi N$ threshold amplitudes at present very difficult. The situation is different in the $\pi\pi$ isospin two final state. Here, the chiral series converges and one finds $a_0^2 = -0.031 \pm 0.007$ consistent with the one-loop chiral perturbation theory prediction.

1 Introduction

Elastic pion–pion scattering in the threshold region is the purest process to test our understanding of the chiral symmetry breaking in QCD. Already in the early days of current algebra, Weinberg [1] showed that the $\pi\pi$ S-wave scattering lengths a_0^I (with $I = 0, 2$ the total isospin of the two-pion system) vanish in the chiral limit of zero quark masses. In particular, he predicted $a_0^0 = 7M_\pi^2/(32\pi F_\pi^2) = 0.16$ and $a_0^2 = (-2/7)a_0^0$. This prediction was further sharpened by Gasser and Leutwyler [2] [3] in the framework of chiral perturbation theory (CHPT), which is the effective field theory of the standard model at low energies. In Ref.[3] a very accurate prediction for the isospin zero, S-wave scattering length was given, $a_0^0 = 0.20 \pm 0.01$, which amounts to a 25% increase compared to the current algebra value. The main assumption underlying this result is that the order parameter of the chiral symmetry breaking, $B = - < 0|\bar{q}q|0 > /F_\pi^2$ (with $< 0|\bar{q}q|0 >$ the scalar quark condensate and $F_\pi \simeq 93$ MeV the pion decay constant) is considerably larger than F_π , $B \gg F_\pi$, which follows e.g. from the standard analysis to determine the light quark mass ratios from the Goldstone boson masses. Another scenario, in which the quark condensate is very much smaller and consequently $B \simeq F_\pi$ has been discussed in Refs.[4] [5]. In this approach, the ratio of the average u and d mass to the strange quark mass is decreased, typically $2m_s/(m_u + m_d) < 10$ and the resulting scattering length a_0^0 increases, typically $a_0^0 \geq 0.27$. To settle this very important issue, it is mandatory to determine the $\pi\pi$ S-wave scattering lengths within an accuracy of about 20% (or better). For a review on these topics, see e.g. [6].

It is, however, not straightforward to determine the $\pi\pi$ phase shifts in the threshold region experimentally. A few possible candidates are $K\ell 4$ –decays, pionic molecules or the reaction $\pi N \rightarrow \pi\pi N$. It is this latter process we will be concerned with in the following. To be more precise, consider single pion production in the threshold region and above. Already Weinberg [8] pointed out that the one-pion exchange diagram contains the four-pion vertex (with one pion leg off-shell). This opens two possibilities of extracting the on-shell $\pi\pi$ interaction. First, one can consider peripheral processes at higher energies but low momentum transfer and try to isolate the pion–pole by standard Chew–Low type techniques (for recent work in this direction, see e.g. [7]). Here, we will concentrate on the second way, namely to directly relate the two independent $\pi\pi N$ threshold amplitudes to the scattering lengths a_0^0 and a_0^2 . This approach was pioneered by Olsson and Turner [9] and has been used ever since in most analyses of the threshold $\pi N \rightarrow \pi\pi N$ data. However, the Olsson–Turner approach predates QCD, it is not applicable any more beyond tree level. In particular, in its original formulation a parameter ξ , which is a measure of the type of chiral symmetry breaking, is left free. In QCD, this parameter ξ is exactly zero. A critical discussion of these topics can be found in [10].

On the other hand, over the last few years an impressive series of experiments have measured the total cross section for the processes $\pi N \rightarrow \pi\pi N$ quite close to threshold [11, 12, 13, 14, 15]. Extracted values for the $\pi\pi$ scattering lengths are based on the Olsson–Turner approach with $\xi \neq 0$ [12, 16]. Therefore, it is necessary to work out a more precise relation between the threshold $\pi\pi N$ amplitudes and the $\pi\pi$ S-wave scattering

lengths beyond tree level. A first step in this direction was made in Refs.[17] [18] where an improved low-energy representation accounting for corrections of order M_π to the tree level relations was formulated. This led to novel low-energy theorems, which can be directly compared with the threshold data. Not unexpectedly, one finds a satisfactory description for the channel $\pi^+ p \rightarrow \pi^+ \pi^+ n$ and some significant deviations for the process $\pi^- p \rightarrow \pi^0 \pi^0 n$, reflecting the relative weakness/strength of the pion-pion interaction in a state with isospin two/zero (in the S-wave). Here, we present the results of a calculation to one loop accuracy in heavy baryon chiral perturbation theory (HBCHPT) [19] [20], which accounts for *all* corrections up-to-and-including $\mathcal{O}(M_\pi^2)$ to the tree level result and which is therefore sensitive to the one-loop corrections to the $\pi\pi$ scattering lengths, besides many other contributions.

The paper is organized as follows. In sections 2, 3 and 4 we formulate the problem, give necessary kinematics and discuss briefly the effective Lagrangian that will be used. Section 5 contains the principal results of this paper, namely the Born, one loop and counterterm contributions to the two threshold $\pi\pi N$ amplitudes up-to-and including order M_π^2 . Numerical results are discussed in section 6 and a short summary is given in section 7. Some technicalities are relegated to the appendices.

2 Prelude I: Threshold kinematics for $\pi N \rightarrow \pi\pi N$

Consider the process

$$\pi^a(k) + N(p_1) \rightarrow \pi^b(q_1) + \pi^c(q_2) + N(p_2) , \quad (1)$$

with ' a, b, c ' pion isospin indices. N denotes the nucleon (neutron or proton). At threshold and in the centre-of-mass frame, we have $q_1 = q_2 = (M_\pi, 0, 0, 0)$, with M_π the pion mass. Using the pseudoscalar quark density $P^a(x) = \bar{q}(x)i\gamma_5\tau^a q(x)$ as interpolating pion field, standard LSZ reduction leads to

$$\begin{aligned} & - \int d^4x d^4y \langle N | T[P^a(0)P^b(x)P^c(y)] | N \rangle e^{i(q_1 \cdot x + q_2 \cdot y)} \\ &= \frac{G_\pi^3}{(M_\pi^2 - q_1^2)(M_\pi^2 - q_2^2)(M_\pi^2 - k^2)} T^{\text{off-shell}} , \end{aligned} \quad (2)$$

with G_π defined via

$$\langle 0 | P^a(0) | \pi^b \rangle = \delta^{ab} G_\pi . \quad (3)$$

At threshold, the on-shell amplitude in the $\pi^a N$ centre-of-mass system can be expressed in terms of two threshold amplitudes,

$$T_{\text{cms}}^{\text{on-shell}} \equiv T = i\vec{\sigma} \cdot \vec{k} [D_1(\tau^b \delta^{ac} + \tau^c \delta^{ab}) + D_2 \tau^a \delta^{bc}] . \quad (4)$$

The quantities $D_{1,2}$ in eq.(4) are related to the commonly used amplitudes $\mathcal{A}_{2I, I_{\pi\pi}}$, with I the total isospin of the initial πN system and $I_{\pi\pi}$ the isospin of the two-pion system in the final state, via

$$\mathcal{A}_{32} = \sqrt{10} D_1, \quad \mathcal{A}_{10} = -2D_1 - 3D_2 . \quad (5)$$

What we are after is the chiral expansion of the D_1 and D_2 . It takes the form (with \mathcal{D} a generic symbol for $D_{1,2}$)

$$\mathcal{D} = f_0 + f_1 \mu + f_2 \mu^2 + \dots, \quad \mu \equiv M_\pi/m, \quad (6)$$

modulo logarithms and we have introduced the pion to nucleon mass (m) ratio, μ .

3 Prelude II: Evolution and formulation of the problem

The modulus of the threshold amplitude is determined by the extrapolation of the measured total cross section in the threshold region via

$$|\mathcal{A}(\pi\pi N)|^2 = \lim_{T_\pi \rightarrow T_\pi^{\text{th}}} \frac{\sigma(\pi N \rightarrow \pi\pi N)}{C S (T_\pi - T_\pi^{\text{th}})^2} \quad (7)$$

where T_π is the incident laboratory pion kinetic energy, S is a Bose symmetry factor ($S = 1/2$ if the final two pions are identical, otherwise it is unity), and

$$C = M_\pi^2 \left(\frac{1}{128\pi^2} \right) \sqrt{3} (2 + \mu)^{1/2} (2 + 3\mu)^{1/2} (1 + 2\mu)^{-11/2}. \quad (8)$$

The threshold modulus has been obtained in this way for the five charge states initiated by $\pi^\pm p$ [16]. Explicit isospin violation due to the electromagnetic mass differences has been removed through the kinematics of the threshold T_π^{th} value and the threshold amplitude modulus is assumed to be isospin invariant.^{#1} By Watson's theorem [21] the threshold amplitude has the phase of the initial elastic $J^P = \frac{1}{2}^+$ P-wave πN scattering amplitude (up to an overall sign). The threshold production amplitude complex phase is then $\delta_{31} \simeq -4^\circ$ for initial πN isospin 3/2 and $\delta_{11} \simeq 2^\circ$ for initial isospin 1/2, as given by the respective phases evaluated at the cms momentum of 213.6 MeV (the $\pi\pi N$ threshold). The threshold production amplitudes are thus nearly real. At threshold the final $\pi\pi$ S-wave state must have isospin 0 or 2 by extended Bose symmetry and hence there are only two independent threshold amplitudes as discussed before. From the measured process amplitude moduli a unique value of \mathcal{A}_{10} and \mathcal{A}_{32} can be found up to an overall sign. We note that the sign is fixed by the chiral expansion (as discussed below).

In the Olsson–Turner approach [9] (with $\xi = 0$), it follows that

$$\begin{aligned} \mathcal{A}_{32} &= -2\sqrt{10}\pi \frac{g_{\pi N}}{m} \left[\frac{a_0^2}{M_\pi^2} + d_2 \right] \\ \mathcal{A}_{10} &= 4\pi \frac{g_{\pi N}}{m} \left[\frac{a_0^0}{M_\pi^2} + d_0 \right] \end{aligned} \quad (9)$$

with $g_{\pi N} = 13.4$ the strong pion–nucleon coupling constant. The above result is a consequence of the dominance of the pion exchange and contact diagrams. To lowest order,

^{#1}A more systematic study of isospin violation is certainly needed.

the two “shift” constants d_I arise from the “sub-leading” diagrams involving three pion absorptions/emissions on the nucleon line, compare Fig. 1. The d_I are of order $\mathcal{O}(M_\pi)$. In the context of QCD, the relations Eq.(9) are equivalent to the tree level CHPT results if the a_0^I are the tree level $\pi\pi$ scattering lengths à la Weinberg. The improved representation of [17] [18], which is based on the first corrections to the Olsson–Turner result, takes the form

$$\begin{aligned}\mathcal{A}_{32} &= -2\sqrt{10}\pi \frac{g_{\pi N}}{m} \left(1 + \frac{7}{2}\mu\right) \left[\frac{a_0^2}{M_\pi^2} + \tilde{d}_2 M_\pi^2 \right] \\ \mathcal{A}_{10} &= 4\pi \frac{g_{\pi N}}{m} \left(1 + \frac{37}{14}\mu\right) \left[\frac{a_0^0}{M_\pi^2} + \tilde{d}_0 M_\pi^2 \right]\end{aligned}\quad (10)$$

where the new shift constants $\tilde{d}_{0,2}$ have the form

$$\tilde{d}_I = \tilde{d}_I^0 + \tilde{d}_I^1 M_\pi + \tilde{d}_I^2 M_\pi^2 + \dots, \quad I = 0, 2 \quad (11)$$

modulo logs. One notices that the correction of order M_π is comparable in size to the leading term (approximately 40% and 50% for \mathcal{A}_{10} and \mathcal{A}_{32} , respectively). Therefore, it is mandatory to calculate (at least) the coefficients \tilde{d}_I^0 . Also, at that order the one-loop corrections to the S-wave $\pi\pi$ scattering lengths appear [2, 3]. The problem investigated here is thus *nothing but the calculation of the constants \tilde{d}_I^0 in eq.(11)*.

4 Prelude III: Effective Lagrangian

In this section, we will briefly discuss the chiral effective pion–nucleon Lagrangian as well as the pionic one underlying our calculation. Many additional details are spelled out in Refs.[3] [20]. To explore in a systematic fashion the consequences of spontaneous and explicit chiral symmetry breaking of QCD, we make use of baryon chiral perturbation theory (in the heavy mass formulation) [19] (HBCHPT). The nucleons are considered as extremely heavy. This allows to decompose the nucleon Dirac spinor into “large” (H) and “small” (h) components

$$\Psi(x) = e^{-imv \cdot x} \{H(x) + h(x)\}, \quad (12)$$

with v_μ the nucleon four-velocity, $v^2 = 1$, and the velocity eigenfields are defined via $\gamma^\mu H = H$ and $\gamma^\mu h = -h$.^{#2} Eliminating the “small” component field h (which generates $1/m$ corrections), the leading order chiral πN Lagrangian reads

$$\mathcal{L}_{\pi N}^{(1)} = \bar{H} (iv \cdot D + \overset{\circ}{g}_A S \cdot u) H. \quad (13)$$

Here the pions are collected in a $SU(2)$ matrix-valued field $U(x)$

$$U(x) = \frac{1}{F} \left[\sqrt{F^2 - \vec{\pi}(x)^2} + i\vec{\tau} \cdot \vec{\pi}(x) \right] \quad (14)$$

^{#2}The role of v_μ is to single out a particular reference frame [22], here the $\pi^a N$ centre-of-mass frame.

with F the pion decay constant in the chiral limit and the so-called σ -model gauge has been chosen which is of particular convenience for our calculations in the nucleon sector. In eq.(13) $D_\mu = \partial_\mu + \Gamma_\mu$ denotes the nucleon chiral covariant derivative, S_μ is a covariant generalization of the Pauli spin vector, $\overset{\circ}{g}_A$ the nucleon axial vector coupling constant in the chiral limit, $u_\mu = iu^\dagger \nabla_\mu U u^\dagger$, with $u = \sqrt{U}$ and ∇_μ the covariant derivative acting on the pion fields. To leading order, $\mathcal{O}(q)$, one has to calculate tree diagrams from

$$\mathcal{L}_{\pi N}^{(1)} + \frac{F^2}{4} \text{Tr}\{\nabla^\mu U \nabla_\mu U^\dagger + \chi_+\} , \quad \chi_+ = u^\dagger \chi u^\dagger + u \chi^\dagger u \quad (15)$$

where the second term is the lowest order mesonic chiral effective Lagrangian, the non-linear σ -model coupled to external sources. The quantity χ contains the light quark mass \hat{m} and external scalar and pseudoscalar sources (the latter are actually needed to compute correlators of the pseudoscalar quark density as in eq.(2)). Later, we will need the five-pion-nucleon vertex. Expanding u in powers of $\phi = \vec{\tau} \cdot \vec{\pi}/F$ gives

$$u = 1 + \frac{i}{2}\phi - \frac{1}{8}\phi^2 + \frac{i}{16}\phi^3 - \frac{5}{128}\phi^4 + \frac{7i}{256}\phi^5 + \mathcal{O}(\phi^6) , \quad (16)$$

and u_μ follows correspondingly, $u_\mu = i\{u^\dagger, \partial_\mu u\}$.

To one-loop accuracy, i.e. order $\mathcal{O}(q^3)$, one has to consider tree graphs from

$$\mathcal{L}_{\text{eff}} = \mathcal{L}_{\pi N}^{(1)} + \mathcal{L}_{\pi N}^{(2)} + \mathcal{L}_{\pi N}^{(3)} + \mathcal{L}_{\pi\pi}^{(2)} + \mathcal{L}_{\pi\pi}^{(4)} . \quad (17)$$

where the structure of $\mathcal{L}_{\pi N}^{(2)}$ is discussed in detail in [18] and, on a pedagogical level, in [23]. All terms in $\mathcal{L}_{\pi N}^{(2)}$ are finite. The first divergences appear to $\mathcal{O}(q^3)$ in HBCHPT, the corresponding determinant has been worked out by Ecker [24],

$$\mathcal{L}_{\pi N}^{(3,\text{div})} = \sum_{i=1}^{22} b_i \bar{H} O_i H , \quad b_i = b_i^r(\lambda) + \frac{\beta_i}{F^2} L \quad (18)$$

where the O_i are monomials in the fields, λ is the scale of dimensional regularization and the b_i differ by a factor $(4\pi F_\pi)^2$ from the ones in [24], and

$$L = \frac{\lambda^{d-4}}{16\pi^2} \left[\frac{1}{d-4} - \frac{1}{2}(\ln(4\pi) - \gamma_E + 1) \right] , \quad (19)$$

with $\gamma_E = 0.5772$ the Euler–Mascheroni constant. There are also terms in $\mathcal{L}_{\pi N}^{(3)}$ with finite coefficients. The corresponding low-energy constants will be estimated by resonance exchange. It is important to note that some of the terms in $\mathcal{L}_{\pi N}^{(2,3)}$ are simply $1/m$ and $1/m^2$ corrections from the original Dirac Lagrangian, like e.g. $\bar{H} D^2/(2m) H$ (for details, see [20]). $\mathcal{L}_{\pi N}^{(2)}$ contains terms proportional to the low-energy constants c_1, c_2, c_3, c_4 . The latter are related to the πN σ -term and πN scattering lengths as discussed below. In order to restore unitarity in a perturbative fashion, one has to include (pion) loop diagrams. In HBCHPT, there exists a strict one-to-one correspondence between the expansion of

any observable in small external momenta *and* quark masses and the expansion in the number of (pion) loops. In what follows we will work within the one-loop approximation corresponding to chiral power $\mathcal{O}(q^3)$. To obtain all contributions at order q^3 one has to supplement the chiral effective Lagrangian by the additional term $\mathcal{L}_{\pi\pi}^{(4)}$ [3]. It serves to cancel some of the divergences of certain loop diagrams and contains the mesonic low-energy constants $\ell_{1,2,3,4}$. The latter encode information about the chiral corrections to the $\pi\pi$ scattering lengths. We use the following form of $\mathcal{L}_{\pi\pi}^{(4)}$ [27],

$$\begin{aligned} \mathcal{L}_{\pi\pi}^{(4)} = & \frac{\ell_1}{4} (\text{Tr} \nabla_\mu U \nabla^\mu U^\dagger)^2 + \frac{\ell_2}{4} \text{Tr}(\nabla_\mu U \nabla_\nu U^\dagger) \text{Tr}(\nabla^\mu U \nabla^\nu U^\dagger) + \frac{\ell_3}{16} (\text{Tr} \chi_+)^2 \\ & + \frac{\ell_4}{16} \left\{ 2 \text{Tr}(\nabla_\mu U \nabla^\mu U^\dagger) \text{Tr} \chi_+ + 2 \text{Tr}(\chi^\dagger U \chi^\dagger U + \chi U^\dagger \chi U^\dagger) - 4 \text{Tr}(\chi^\dagger \chi) - (\text{Tr} \chi_-)^2 \right\} + \dots \end{aligned} \quad (20)$$

where the ellipsis stands for other terms of order q^4 which do, however, not contribute in our case. The finite pieces ℓ_i^r of the low-energy constants ℓ_i in eq.(20) are renormalization scale dependent and are related to the $\bar{\ell}_i$ of ref.[3] via

$$\begin{aligned} \bar{\ell}_1 &= 96\pi^2 \ell_1^r(\lambda) - 2 \ln \frac{M_\pi}{\lambda} , \quad \bar{\ell}_2 = 48\pi^2 \ell_2^r(\lambda) - 2 \ln \frac{M_\pi}{\lambda} , \\ \bar{\ell}_3 &= -64\pi^2 \ell_3^r(\lambda) - 2 \ln \frac{M_\pi}{\lambda} , \quad \bar{\ell}_4 = 16\pi^2 \ell_4^r(\lambda) - 2 \ln \frac{M_\pi}{\lambda} , \end{aligned} \quad (21)$$

and their actual values will be discussed later. From the Lagrangian eq.(20), one derives the chiral corrections to the S-wave $\pi\pi$ scattering lengths [3] (we do not exhibit the explicit scale-dependence of the ℓ_i^r any more)

$$a_0^0 = \frac{7M_\pi^2}{32\pi F_\pi^2} \left[1 + \left(\frac{M_\pi}{4\pi F_\pi} \right)^2 \left(\frac{5}{2} - 9 \ln \frac{M_\pi}{\lambda} \right) + \frac{2M_\pi^2}{7F_\pi^2} \left(20\ell_1^r + 20\ell_2^r + 5\ell_3^r + 7\ell_4^r \right) \right] \quad (22)$$

$$a_0^2 = -\frac{M_\pi^2}{16\pi F_\pi^2} \left[1 + \left(\frac{M_\pi}{4\pi F_\pi} \right)^2 \left(3 \ln \frac{M_\pi}{\lambda} - \frac{1}{2} \right) + \frac{2M_\pi^2}{F_\pi^2} \left(-4\ell_1^r - 4\ell_2^r - \ell_3^r + \ell_4^r \right) \right] \quad (23)$$

with M_π and F_π the empirical values (i.e. the corresponding chiral corrections have been accounted for, see also [28]). We have now assembled all tools for calculating the one loop corrections for $\pi N \rightarrow \pi\pi N$.

5 $\pi N \rightarrow \pi\pi N$ to one loop

Before presenting the results of the calculation, some general remarks are in order. The various contributions to the chiral expansion of the invariant functions $D_{1,2}$ to order q^3 can be grouped as

$$\mathcal{D}^{(3)} = \mathcal{D}^{\text{Born}} + \mathcal{D}^{\text{one-loop}} + \mathcal{D}^{\text{ct}} , \quad (24)$$

where $\mathcal{D}^{\text{Born}}$ subsumes the lowest order relativistic tree graphs and all kinematical corrections to it (which are suppressed by powers of $1/m$), $\mathcal{D}^{\text{one-loop}}$ the generic one loop graphs

and \mathcal{D}^{ct} the counter terms, which absorb the divergences from the loops and there are, of course, additional finite ones. At threshold, the calculation simplifies since we have the selection rules

$$S \cdot q_1 = S \cdot q_2 = v \cdot (q_1 - q_2) = 0, \quad v \cdot q_1 = v \cdot q_2 = M_\pi \quad v \cdot k = 2M_\pi + \mathcal{O}(\frac{1}{m}). \quad (25)$$

Also, from the start we will perform mass and coupling constant renormalization, as explained in the context of the Born graphs (see below). We will give a fairly detailed description of the renormalization of the remaining divergences since that will serve as an excellent check on the calculations. Furthermore, the extraction of the various low-energy constants and a thorough discussion of the related uncertainties is mandatory to really filter out the sensitivity of the threshold $\pi\pi N$ amplitudes to the S-wave $\pi\pi$ scattering lengths.

5.1 Renormalized Born terms

From the three-pion-nucleon seagull and the pion-pole diagram,^{#3} one immediately finds the leading $\mathcal{O}(q)$ contribution to $D_{1,2}$

$$D_1 = \frac{\overset{\circ}{g}_A}{8F^3}, \quad D_2 = -\frac{3\overset{\circ}{g}_A}{8F^3}. \quad (26)$$

It is then most economic to calculate the relativistic tree graphs and expand the result in powers of μ , see Fig. 1. This gives automatically all kinematical corrections to eq.(26) and reads to order $\mathcal{O}(q^3)$

$$D_1^{\text{Born}} = \frac{\overset{\circ}{g}_A}{8F^3} \left[1 + \frac{7}{2}\mu - \mu^2 \left(\frac{1}{8} + \frac{3}{2}g_A^2 \right) \right], \quad D_2^{\text{Born}} = \frac{\overset{\circ}{g}_A}{8F^3} \left[-3 - \frac{17}{2}\mu + \mu^2 \left(\frac{11}{8} + 2g_A^2 \right) \right]. \quad (27)$$

In what follows, we have to renormalize the factor $\overset{\circ}{g}_A / F^3$ (i.e. the chiral limit value) to the physical value $g_{\pi N}/(mF_\pi^2)$. This renormalization procedure subsumes a host of loop and counter term corrections. For doing that, we first have to consider the pion mass, decay constant and so on [3]. To one loop we have for the pseudoscalar coupling G_π (cf. Fig. 2)

$$G_\pi = G \left[1 + \frac{M^2}{F^2} \left(2\ell_3^r + \ell_4^r - \frac{1}{16\pi^2} \ln \frac{M}{\lambda} \right) \right], \quad (28)$$

with G the chiral limit value of G_π . Similarly, we find for the pion decay constant

$$F_\pi = F \left[1 + \frac{M^2}{F^2} \left(\ell_4^r - \frac{1}{8\pi^2} \ln \frac{M}{\lambda} \right) \right], \quad (29)$$

^{#3} It is important to remark that this splitting has no physical meaning. The contributions of the threshold amplitudes $D_{1,2}$ coming from the seagull and the pion pole depend on the choice of interpolating pion field, i.e. how one parametrizes $U(x)$ through some pion field. The sum as a physical quantity is of course unique and independent of the particular choice.

and the pion mass renormalization reads

$$M_\pi^2 = M^2 \left[1 + \frac{M^2}{F^2} \left(2\ell_3^r + \frac{1}{16\pi^2} \ln \frac{M}{\lambda} \right) \right], \quad (30)$$

with $M^2 = 2\hat{m}B$ the leading term in the quark mass expansion of the pion mass squared. With that, the pion propagator takes the form (in the σ -model gauge),

$$\frac{i Z_\pi}{q^2 - M_\pi^2}, \quad Z_\pi = 1 - \frac{M^2}{F^2} \left[2L + 2\ell_4 + \frac{1}{8\pi^2} \ln \frac{M}{\lambda} \right]. \quad (31)$$

The pertinent diagrams contributing to the renormalization of the pion–nucleon vertex are shown in Fig. 3. The appropriate one-loop graphs for $\pi N \rightarrow \pi\pi N$ which account for this renormalization will have to be identified and subtracted accordingly, see the next section. The coupling constant renormalization can be written as

$$\frac{g_{\pi N}}{m} = \frac{g_A}{F_\pi} \left(1 - \frac{2b_{11}M_\pi^2}{F_\pi^2} \right), \quad (32)$$

where the constant b_{11} is finite. Its value is fixed from the known Goldberger–Treiman discrepancy. However, there remains a finite contribution to $D_{1,2}$ from the corresponding chiral power three Lagrangian,

$$\mathcal{L}_{\pi N}^{(3)} = b_{11} \frac{g_A}{F_\pi^2} \bar{H} iS \cdot (D\chi_-) H, \quad (33)$$

after the $g_{\pi N}$ renormalization, eq.(32), has been performed,

$$D_1^{\text{GTR}} = 0, \quad D_2^{\text{GTR}} = -g_A b_{11} \frac{M_\pi^2}{F_\pi^5}. \quad (34)$$

This has to be accounted for.

5.2 One loop graphs

In Fig. 4, we show the 36 different one-loop diagrams that contribute at threshold (we do not display graphs in which the two out-going pions are interchanged, $b \leftrightarrow c$). We have made use of the selection rules, eq.(25), and omitted all those diagrams which according to these rule are equal to zero. This means that if one wants to extend this calculation to kinematics above threshold, one has to consider many more diagrams than shown in Fig. 4 since then the selection rules do not apply anymore. Of course, many of the graphs shown contribute to mass and coupling constant renormalization. Concerning the chiral corrections to the pion-pion interaction, the interesting diagrams are the ones numbered 16, 17 and 18. The calculation of all these diagrams is straightforward but somewhat tedious. It is most economically done in the basis of the loop functions defined in appendix B of ref.[18]. In appendix A, we assemble some novel loop functions not considered in [18].

Putting all pieces together, one has (after renormalization of F_π , G_π and $g_{\pi N}$),

$$D_1^{\text{loop}} = \frac{g_A M_\pi^2}{32\pi^2 F_\pi^5} \left[\left(g_A^2 - \frac{1}{4} \right) \ln \frac{M_\pi}{\lambda} - \frac{25}{24} + \frac{g_A^2}{6} + \left(\frac{g_A^2}{2} - \frac{7}{8} \right) \sqrt{3} \ln(2 + \sqrt{3}) - i \frac{\pi}{4} \sqrt{3} g_A^2 + 10 I \right] \\ + \frac{g_A M_\pi^2}{F_\pi^5} \left[\frac{g_A^2}{2} - \frac{1}{8} \right] L , \quad (35)$$

$$D_2^{\text{loop}} = \frac{g_A M_\pi^2}{32\pi^2 F_\pi^5} \left[\left(\frac{43}{4} - 10g_A^2 \right) \ln \frac{M_\pi}{\lambda} - \frac{73}{24} + \frac{16g_A^2}{3} - \left(5g_A^2 - \frac{1}{2} \right) \sqrt{3} \ln(2 + \sqrt{3}) + i \frac{5\pi}{2} \sqrt{3} g_A^2 + 4 I \right] \\ + \frac{g_A M_\pi^2}{F_\pi^5} \left[\frac{43}{8} - 5g_A^2 \right] L , \quad (36)$$

with

$$I = \int_0^1 dx \frac{x}{\sqrt{(1-x)(1+3x)}} \arctan \frac{x}{\sqrt{(1-x)(1+3x)}} = 0.6456 . \quad (37)$$

The imaginary part in eqs.(35,36) is due to the diagrams numbered 20, 21, 24, ..., 28. For these pion–nucleon rescattering type of graphs, the pertinent loop functions have to be evaluated at $\omega = 2M_\pi$, which is well above the branch point $\omega_0 = M_\pi$. This is similar to the effect observed in the calculation of the threshold amplitudes for the reaction $\gamma N \rightarrow \pi\pi N$, where one also finds an imaginary part at threshold [25]. If one calculates from eqs.(35,36) the imaginary parts of the isospin amplitudes \mathcal{A}_{10} and \mathcal{A}_{32} and compares them to those demanded by Watson’s theorem (using the experimental fit values for the real parts), one makes the following observation. The phase is approximately correct for the isospin 3/2 case but an order of magnitude too large with the wrong sign in the isospin 1/2 case. The reason for this is that the tree level phases which we encounter here satisfy $\delta_{11} = 4\delta_{31}$ which does not hold for the empirical $P_{2I,1}$ phase at the $\pi\pi N$ threshold. Nevertheless, the appearance of the tree level πN phases in eqs.(35,36) serves as a good check on the one-loop calculation. We encounter here the standard problem in chiral perturbation theory that for getting the imaginary parts better, one has to perform a higher order calculation. As discussed in the introduction, $D_{1,2}$ have to be almost real, therefore we will neglect in the following their imaginary parts. Next, we have to perform the remaining renormalizations to get rid of the terms proportional to L .

5.3 Renormalization

We proceed in two steps. First, we consider the divergences related to the pion–nucleon Lagrangian $\mathcal{L}_{\pi N}^{(3)}$, eq.(18). The following operators as defined in Ref.[24] give a non–vanishing contribution at threshold; $O_4, O_5, O_6, O_7, O_9, O_{17}, O_{18}$ and O_{20} . Some of these are equivalent at threshold, these are O_4 and O_6 , O_5 and O_7 and the combination of O_{17} plus O_{18} . The corresponding β ’s are $\beta_5 + \beta_7 = g_A(1 - g_A^2)/2$, $\beta_4 + \beta_6 = -g_A/2$ and $\beta_{17} + \beta_{18} = (2 - 3g_A^2)/4$. The operator $O_9 = S \cdot u \text{Tr}(\chi_+)$ has two terms with three pion fields. First, there is a three–pion vertex from u_μ . This contribution is, however, completely contained in the renormalization of $g_{\pi N}$. Second, there is a term with one

pion from u_μ and two from $\text{Tr}(\chi_+)$ with $\beta_9 = g_A(4 - g_A^2)/8$. Finally, there is the operator $O_{20} = iv \cdot D\text{Tr}(\chi_+) + \text{h.c.}$. The relevant contribution has a vertex with two pions coming from $\text{Tr}(\chi_+)$ with $\beta_{20} = -9g_A^2/16$. Adding up all these counterterm contributions which in the case of O_{17} , O_{18} and O_{20} come from two step processes with a $\sigma \cdot k$ interaction for the incoming pion π^a , we have (the scale-dependence of the b_i^r is not made explicit)

$$D_1^{(\text{ct},3)} = \frac{M_\pi^2}{F_\pi^3} \left[b_5^r + b_7^r + \frac{g_A}{2F_\pi^2} (1 - g_A^2) L \right], \quad (38)$$

$$D_2^{(\text{ct},3)} = \frac{M_\pi^2}{F_\pi^3} \left[2(b_4^r + b_6^r + b_9^r) - 4g_A(b_{17}^r + b_{18}^r + b_{20}^r) + \frac{g_A}{F_\pi^2} (5g_A^2 - 2) L \right], \quad (39)$$

where the terms $\sim g_A^3 L$ are cancelled by the infinities in D_1^{loop} and D_2^{loop} , eqs.(35,36), respectively. So we are left with the following divergent pieces:

$$D_1^{\text{div,loop+ct3}} = \frac{g_A M_\pi^2}{F_\pi^5} \left(\frac{3}{8} L \right), \quad D_2^{\text{div,loop+ct3}} = \frac{g_A M_\pi^2}{F_\pi^5} \left(\frac{27}{8} L \right), \quad (40)$$

which have to be cancelled by the counter terms from $\mathcal{L}_{\pi\pi}^{(4)}$. After renormalization of F_π , G_π and $g_{\pi N}$, the total contribution from $\mathcal{L}_{\pi\pi}^{(4)}$ reads

$$D_1^{(\text{ct},4)} = \frac{g_A M_\pi^2}{F_\pi^5} \left[-\frac{3}{8} L - \frac{3}{2} \ell_2^r - \frac{1}{4} \ell_3^r + \frac{1}{4} \ell_4^r \right], \quad (41)$$

$$D_2^{(\text{ct},4)} = \frac{g_A M_\pi^2}{F_\pi^5} \left[-\frac{27}{8} L - 3 \ell_1^r - \frac{1}{4} \ell_3^r - \frac{5}{4} \ell_4^r \right]. \quad (42)$$

We remark that the low-energy constant ℓ_3 does only appear via the renormalization of the pion mass with the appropriate insertion from $\mathcal{L}_{\pi\pi}^{(4)}$ for the pion hooking on to the nucleon (cf. graph 12 in Fig.4) since $[\text{Tr}(\chi_+)]^2$ has no four-pion vertex in the σ -model gauge.^{#4} Comparison of eqs.(41,42) with eq.(40) leads to the desired result, namely

$$D_i^{\text{div}} = D_i^{\text{div,loop}} + D_i^{\text{div,3}} + D_i^{\text{div,4}} = 0, \quad i = 1, 2. \quad (43)$$

This cancellation of divergences serves as an important check on our calculation. The finite counter term contribution can be compactly written as

$$D_1^{\text{ct,fin}} = \frac{M_\pi^2}{F_\pi^3} \left[\frac{g_A}{F_\pi^2} \left(\frac{\ell_4^r}{4} - \frac{\ell_3^r}{4} - \frac{3}{2} \ell_2^r \right) + \delta_1^r \right], \quad (44)$$

$$D_2^{\text{ct,fin}} = \frac{M_\pi^2}{F_\pi^3} \left[-\frac{g_A}{F_\pi^2} \left(3 \ell_1^r + \frac{5}{4} \ell_4^r + \frac{1}{4} \ell_3^r \right) + \delta_2^r \right], \quad (45)$$

where the $\delta_{1,2}^r$ subsume the appropriate contributions of the b_i^r plus additional finite pieces from $\mathcal{L}_{\pi N}^{(3)}$ and from $1/m$ suppressed corrections from $\mathcal{L}_{\pi N}^{(2)}$. The estimation of these finite pieces will be discussed in the next section.

^{#4}We have checked that in other parametrizations of U where $[\text{Tr}(\chi_+)]^2$ has a four-pion vertex, the final result is the same.

5.4 Finite contributions and estimation of low-energy constants

The most difficult task is to pin down the finite terms $\delta_{1,2}^r$ in eqs.(44,45). These can be split into two distinct contributions. First, there are $1/m$ suppressed terms with insertions from the relativistic chiral order two Lagrangian $\mathcal{L}_{\pi N}^{(2)}$. In Ref.[17] we had already shown that such terms cancel at order M_π^2 which allowed to formulate low-energy theorems for $D_{1,2}$ independent of the corresponding low-energy constants c_i . Here, we are working one order further and thus such contributions appear, some examples are shown in Fig.5. These are operators of dimension three which contribute at threshold. The other type of terms are related to the values of the various $b_i^r(\lambda)$ due to the renormalization and additional finite ones from $\mathcal{L}_{\pi N}^{(3)}$. In the absence of a complete data set to fit these, we will make use of the resonance saturation principle. This procedure will induce some uncertainty in our final results, see the discussions in [18] and [26]. The exception to this is the term $\sim b_{11}$ discussed in section 5.1. This particular contribution can not be explained by resonance exchange.

Consider first the contributions due to insertions from $\mathcal{L}_{\pi N}^{(2)}$. These can be either calculated by performing the path integral as in ref.[20] and expanding to the desired order, or, more economically, by using the relativistic Lagrangian $\mathcal{L}_{\pi N}^{(2,rel)}$. It is this latter method we are using.^{#5} It is same method used in the calculation of the $1/m$ suppressed (kinematical) corrections to the tree graphs, compare section 5.1. It is based on the observation that all operators which have fixed coefficients like $1/m$, $1/m^2$, g_A/m , and so on are nothing but the expansion coefficients of the relativistic theory (see e.g. Refs.[20],[23]). The corresponding dimension two effective relativistic pion–nucleon Lagrangian reads [27] [29]

$$\begin{aligned} \mathcal{L}_{\pi N}^{(2,rel)} = & c_1 \bar{\Psi} \Psi \text{Tr}(\chi_+) + \frac{c'_2}{4m} \bar{\Psi} i \gamma_\mu \overset{\leftrightarrow}{D}_\nu \Psi \text{Tr}(u^\mu u^\nu) - \frac{c''_2}{8m^2} \bar{\Psi} \overset{\leftrightarrow}{D}_\mu \overset{\leftrightarrow}{D}_\nu \Psi \text{Tr}(u^\mu u^\nu) \\ & + c_3 \bar{\Psi} u_\mu u^\mu \Psi + c_4 \frac{i}{4} \bar{\Psi} \sigma_{\mu\nu} [u^\mu, u^\nu] \Psi + \dots \end{aligned} \quad (46)$$

where Ψ denotes the relativistic nucleon field and the ellipsis stands for other terms not needed here. The c_i are normalized such that we can identify them with the corresponding low-energy constants of the heavy baryon Lagrangian (truncated at order q^2) (for definitions, see e.g. [18]). Note that the constants c'_2 and c''_2 are related to the c_4 and c_5 of App. A in [20] and that they have been renamed in comparison to Ref.[27]. To leading order in the heavy baryon Lagrangian, we have $c_2 = c'_2 + c''_2$ in the notation of Ref.[18]. The contribution of these terms to the $D_{1,2}$ follows as,

$$D_1^{(c_i)} = \frac{g_A M_\pi^2}{m F_\pi^3} \left(-2c_1 + \frac{3}{2} c'_2 + 2c''_2 + 2c_3 + \frac{1}{2} c_4 \right), \quad (47)$$

$$D_2^{(c_i)} = -\frac{g_A M_\pi^2}{m F_\pi^3} \left(c'_2 + 2c''_2 + c_4 \right). \quad (48)$$

^{#5}In appendix C, we derive the result for $D_{1,2}$ directly from the path-integral formulation of the heavy-nucleon Lagrangian.

For the numerical evaluation of the c_i and to the accuracy we are working, we can fix them to order q^2 (i.e. just calculating tree graphs) from available pion–nucleon scattering data. Therefore, the values presented here will differ from previous estimates which included q^3 contributions. This difference is, of course, just one of the many corrections of $\mathcal{O}(M_\pi^3)$ in D_1 and D_2 and only becomes important if one wants to extend the calculation presented here to the next order. First, we invoke the subthreshold expansion of the standard invariant pion–nucleon amplitudes with the pseudovector Born terms subtracted (as indicated by the 'bar') [30]

$$\bar{X} = \sum_{m,n} x_{m,n} \nu^{2m+k} t^n, X = \{A^+, B^+, A^-, B^-\}, \quad (49)$$

with t the invariant momentum transfer squared, $\nu = (s - u)/4m$ (s, t, u are the conventional Mandelstam variables subject to the constraint $s + t + u = 2M_\pi^2 + 2m^2$) and $k = 1$ (0) if the function considered is odd (even) in ν . Retaining terms to order $\mathcal{O}(\nu^2, t)$, one finds from eq.(46)

$$\begin{aligned} \bar{A}^+ &= -\frac{4c_1 M_\pi^2}{F_\pi^2} + \frac{c_3}{F_\pi^2} (2M_\pi^2 - t) + \frac{2c_2''}{F_\pi^2} \nu^2, \quad \bar{B}^+ = \frac{2c_2'}{F_\pi^2} \nu, \\ \bar{A}^- &= -\frac{2mc_4}{F_\pi^2} \nu, \quad \bar{B}^- = \frac{1}{2F_\pi^2} + \frac{2c_4 m}{F_\pi^2}, \end{aligned} \quad (50)$$

where the first term in \bar{B}^- stems from the celebrated Weinberg–Tomozawa term [1] [31]. From that, we deduce the following relations to order q^2 ,

$$\begin{aligned} a_{00}^+ &= \frac{2M_\pi^2}{F_\pi^2} (c_3 - 2c_1), \quad a_{00}^- = -\frac{2mc_4}{F_\pi^2}, \quad a_{10}^+ = \frac{2c_2''}{F_\pi^2}, \quad a_{01}^+ = -\frac{c_3}{F_\pi^2}, \\ b_{00}^+ &= \frac{2c_2'}{F_\pi^2}, \quad b_{00}^- = \frac{1}{2F_\pi^2} (1 + 4c_4 m). \end{aligned} \quad (51)$$

Further information is obtained for c_1 from the πN – σ term [20] [27], $\sigma_{\pi N}(0) = -4c_1 M_\pi^2$ (to order q^2) and for c_3 and c_4 from the wave scattering volumina c_0 and d_1 ,

$$c_0 = -\frac{c_3}{2\pi F_\pi^2}, \quad d_1 = -\frac{1}{4\pi F_\pi^2} \left(c_4 + \frac{1}{4m} \right). \quad (52)$$

We are left with terms related to $\mathcal{L}_{\pi N}^{(3)}$. There is the finite contribution from the pion–nucleon vertex renormalization as discussed in section 5.1. It leads to $D_{1,2}^{\text{GTR}}$ as given in eq.(34). The remaining contributions will be estimated by resonance exchange. This works well in the meson sector [32], it is, however, more complicated in the baryon case since one can have excited nucleon intermediate states as well as scalar and vector meson couplings to two or three pions. For our case, we estimate the genuine counter terms from $\mathcal{L}_{\pi N}^{(3)}$ via single and double N^* excitations and meson exchange, see Fig. 6. Notice that at threshold, the vector meson contribution analogous to the scalar meson one vanishes.

To be precise, the ρ has a P-wave coupling and the $3\pi\omega$ vertex vanishes at threshold. In principle, there could also be a contribution due to the a_1 3 π coupling. However, the branching ratio $a_1 \rightarrow (\pi\pi)_S\pi$ is so small that we can safely neglect this contribution. We now turn to the non-vanishing parts. First, we consider the $\Delta(1232)$. If one treats it non-relativistically, all graphs with double- Δ excitations vanish at threshold, as it is e.g. the case in the model of ref.[35]. These diagrams are obviously of order q^3 and proportional to \vec{q}_i , which vanishes at threshold. Relativistically, the double- Δ graphs first contribute at order M_π^3 to $D_{1,2}$.

Second, there is the Roper, $N^*(1440)$. It has a very large width for decaying into a nucleon and two pions. The corresponding Lagrangian $\mathcal{L}_{N^*N\pi\pi}$ for S-wave emission is discussed in detail in appendix B since in the available literature it is not treated in its most generality (as needed here). On the other hand, $\mathcal{L}_{N^*N\pi}$ is standard,

$$\mathcal{L}_{N^*N\pi} = \frac{g_A}{4} \sqrt{R} \bar{\Psi}_{N^*} \gamma_\mu \gamma_5 u^\mu \Psi_N + \text{h.c.} , \quad (53)$$

with $\sqrt{R} = 0.53 \pm 0.04$ from the total width [34] (calculated relativistically).^{#6} Putting pieces together, the Roper contribution is

$$D_1^{N^*} = 0 , \quad D_2^{N^*} = \frac{(c_1^* + c_2^*) g_A \sqrt{R} M_\pi^2}{F_\pi^3 (m^* - m)} . \quad (54)$$

The coupling constant combination $c_1^* + c_2^* = -1.56 \pm 3.35 \text{ GeV}^{-1}$ follows from the partial width $\Gamma(N^* \rightarrow N(\pi\pi)_S)$ with both pions in an S-state [33]. The details can be found in appendix B.

The next resonance which decays into a nucleon and two pions is the $D_{13}(1520)$. Non-relativistically, this D-wave state cannot be excited by the initial P-wave πN system and thus we neglect such a possible contribution. Of course, at energies above threshold such resonances become important, as witnessed e.g. by the study of the reaction $\gamma p \rightarrow \pi^+ \pi^- p$ in [36]. We remark that our treatment of the baryon resonance contributions is in good agreement with the partial wave-analysis of $\pi N \rightarrow \pi\pi N$ by Manley et al. [37]. In their table VI one sees that at the lowest energy considered, only the Roper leads to a sizeable cross section. There is no sign of the Δ and the D_{13} contribution is approximately one order of magnitude smaller than the one from the P_{11} . This lends further credit to our argument of exclusively keeping the Roper excitation to estimate the baryon resonance contribution to the threshold $\pi\pi N$ amplitudes. Third, there is scalar meson exchange. Its main contribution comes from diagrams with a nucleon pole. This is supposedly contained in the empirical values of the c_i , as discussed in some detail in Refs.[18] [26]. The remaining terms are of the form depicted in Fig. 6c and include the vertex πSNN . In the absence of any empirical indication about the strength of this coupling constant and the lack of theoretical models thereof, we will set such terms to zero. It is conceivable that this is a good approximation since the bulk of scalar meson exchange is expected to be encoded in some of the terms proportional to the constants c_i .

^{#6}We use here the width as obtained from the speed plot, not the model-dependent Breit-Wigner fits, $\Gamma_{\text{tot}} = 160 \pm 40 \text{ MeV}$ [34] and as branching ratios $\text{BR}(N^* \rightarrow N\pi) = 0.68$ and $\text{BR}(N^* \rightarrow N(\pi\pi)_S) = 0.075 \pm 0.025$ [33].

5.5 The master formula

We have now assembled all pieces to give the chiral expansion of the threshold amplitudes $D_{1,2}$, or equivalently, \mathcal{A}_{10} and \mathcal{A}_{32} . The chiral corrections to the amplitudes $D_{1,2}$ follow by combining eqs.(27,34,35,36,47,48, 54). We have

$$D_i = D_i^{\text{LET}} + D_i^{(2)} + \mathcal{O}(M_\pi^3) , \quad i = 1, 2 , \quad (55)$$

with

$$D_1^{\text{LET}} = \frac{g_{\pi N}}{8mF_\pi^2} \left(1 + \frac{7}{2}\mu \right) , \quad D_2^{\text{LET}} = -\frac{g_{\pi N}}{8mF_\pi^2} \left(3 + \frac{17}{2}\mu \right) , \quad (56)$$

and we do not write down again the various pieces contributing to the order M_π^2 corrections explicitly. Symbolically, they take the form

$$D_i^{(2)} = D_i^{(2,\text{Born})} + D_i^{(2,\text{loop})} + D_i^{(2,\ell_i)} + D_i^{(2,c_i)} + D_i^{(2,\text{GTR})} + D_i^{(2,N^*)} , \quad i = 1, 2 , \quad (57)$$

with $D_1^{(2,\text{GTR})} = D_1^{(2,N^*)} = 0$, and we neglect the imaginary parts as discussed before. The LETs were first derived in ref.[17]. With the help of eqs.(22,23) as well as eq.(5), we can make explicit the $\pi\pi$ scattering lengths (i.e. give the constants \tilde{d}_I^0 , cf. eq.(11)). This determines the relation between the threshold $\pi\pi N$ amplitudes and the $\pi\pi$ scattering lengths one order beyond the improved representation, eq.(10), and reads,

$$\text{Re } \mathcal{A}_{10} = 4\pi \frac{g_{\pi N}}{m} \frac{a_0^0}{M_\pi^2} + \frac{37g_{\pi N}M_\pi}{16m^2F_\pi^2} + \Delta_0 \frac{g_A M_\pi^2}{32F_\pi^5} + \mathcal{O}(M_\pi^3) \quad (58)$$

$$\text{Re } \mathcal{A}_{32} = -2\sqrt{10}\pi \frac{g_{\pi N}}{m} \frac{a_0^2}{M_\pi^2} + \frac{7\sqrt{10}g_{\pi N}M_\pi}{16m^2F_\pi^2} + \Delta_2 \frac{\sqrt{10}g_A M_\pi^2}{128F_\pi^5} + \mathcal{O}(M_\pi^3) \quad (59)$$

with

$$\begin{aligned} \Delta_0 = & 16 \left(8\ell_1^r - 4\ell_2^r + 3\ell_4^r \right) - \frac{F_\pi^2}{m^2} \left(\frac{31}{2} + 12g_A^2 \right) + \frac{64F_\pi^2}{m} \left(2c_1 - 2c_3 + c_4 + c_2'' \right) + \\ & \frac{1}{\pi^2} \left[(28g_A^2 - 16) \ln \frac{M_\pi}{\lambda} + \frac{41}{6} - \frac{49}{3}g_A^2 + (14g_A^2 + \frac{1}{4})\sqrt{3} \ln(2 + \sqrt{3}) - 32I \right] \\ & + 96 \left(-(c_1^* + c_2^*)\sqrt{R} \frac{F_\pi^2}{m^* - m} + b_{11} \right) \end{aligned} \quad (60)$$

$$\begin{aligned} \Delta_2 = & 32 \left(4\ell_1^r - 2\ell_2^r \right) - \frac{2F_\pi^2}{m^2} (1 + 12g_A^2) + \frac{64F_\pi^2}{m} \left(-4c_1 + 4c_3 + c_4 + 3c_2' + 4c_2'' \right) + \\ & \frac{1}{\pi^2} \left[(4g_A^2 - 4) \ln \frac{M_\pi}{\lambda} + \frac{1}{3}(2g_A^2 - 11) + (2g_A^2 - \frac{7}{2})\sqrt{3} \ln(2 + \sqrt{3}) + 40I \right] \end{aligned} \quad (61)$$

where the factors in front of $\Delta_{0,2}$ have been chosen such that the $\Delta_{0,2}$ are numerically of the order $\mathcal{O}(1)$ and I is given in eq.(37). For the discussion of the respective numerical values, we abbreviate the $\mathcal{O}(M_\pi^2)$ contributions as follows,

$$\Delta_{0,2} = \Delta_{0,2}^{\ell_i} + \Delta_{0,2}^{\text{Born}} + \Delta_{0,2}^{c_i} + \Delta_{0,2}^{\text{loop}} + \Delta_{0,2}^{\text{ct3}} , \quad (62)$$

where the various terms can be read off from eqs.(60,61). Obviously, $\Delta_2^{\text{ct3}} = 0$.

6 Results and discussion

First, we must fix parameters. Throughout, we use $F_\pi = 93$ MeV, $M_\pi = 139.57$ MeV, $m = 938.27$ MeV, $g_{\pi N} = 13.4$, $g_A = 1.26$ and $m^* = 1440$ MeV. This leads to $b_{11} = -0.012$.

Consider the low-energy constants c_i . From the formulae given in section 5.4 and with the empirical information contained in table 2.4.7.1 of [30], together with $\sigma_{\pi N}(0) = 45 \pm 9$ MeV [38] and the scattering volumina $c_0 = (0.208 \pm 0.003) M_\pi^{-3}$ and $d_1 = (-0.069 \pm 0.002) M_\pi^{-3}$ [30], we arrive at the numbers given in table 1. We note that these numbers are typically a factor 1.5 smaller than the ones from the determination including the loop effects at order q^3 [18]. The uncertainty in the table reflects the spread of the various determinations (to order q^2) if possible (like for c_1 , c_3 and c_4), otherwise the uncertainty of the empirical input.

c_1	c'_2	c''_2	c_3	c_4
-0.64 ± 0.14	-5.63 ± 0.10	7.41 ± 0.10	-3.90 ± 0.09	2.25 ± 0.09

Table 1: The low-energy constants c_i . All values in GeV^{-1} .

From these numbers, we deduce

$$\Delta_0^{c_i} = 9.54 \pm 0.21, \quad \Delta_2^{c_i} = 1.16 \pm 0.50. \quad (63)$$

Next, we need the low-energy constants from the meson sector, $\ell_{1,2,3,4}^r$. We take the $\bar{\ell}_{1,2}$ from the recent analysis of $K_{\ell 4}$ data beyond one loop [39] and the $\ell_{3,4}$ from the classical paper [3],

$$\begin{aligned} 10^3 \ell_1^r(1\text{GeV}) &= -5.95 \pm 1.06, & 10^3 \ell_2^r(1\text{GeV}) &= 4.35 \pm 2.75, \\ 10^3 \ell_3^r(1\text{GeV}) &= 1.64 \pm 3.80, & 10^3 \ell_4^r(1\text{GeV}) &= 2.29 \pm 5.70, \end{aligned} \quad (64)$$

leading to

$$\Delta_0^{l_i} = -0.93 \pm 0.40, \quad \Delta_2^{l_i} = -1.04 \pm 0.22. \quad (65)$$

at the scale $\lambda = 1$ GeV. If one lets λ run from 0.5 to 1.5 GeV, one finds $\Delta_0^{l_i} = -0.49 \dots -1.05$ and $\Delta_2^{l_i} = -1.06 \dots -0.98$. To account for this, we scale up the uncertainty of $\Delta_0^{l_i}$ by a factor 1.5. The Born contribution to $\Delta_{0,2}$ is small, we find

$$\Delta_0^{\text{Born}} = -0.34, \quad \Delta_2^{\text{Born}} = -0.39. \quad (66)$$

The corresponding loop contributions are also readily evaluated,

$$\Delta_0^{\text{loop}} = -4.48 \pm 1.58, \quad \Delta_2^{\text{loop}} = 1.81 \pm 0.16. \quad (67)$$

for $\lambda = 1$ GeV as the central value and the uncertainty accounts for the variation if λ varies from 0.5 to 1.5 GeV. To end this part, we give the GTR and Roper contributions,

$$\Delta_0^{\text{ct3}} = \Delta_0^{\text{GTR}} + \Delta_0^{N^*} = 0.22 \pm 3.58, \quad (68)$$

where the large uncertainty stems from the Roper couplings $c_1^* + c_2^*$. From these numbers we can already conclude that the $1/m$ corrections to the πN scattering amplitude ($\sim \Delta_{0,2}^{c_i}$) play a dominant role in the total correction of order M_π^2 together with the Roper excitation. Also, if one separates out the $\pi\pi$ interactions, their contribution is comparably small. This indicates that a very accurate determination of the S-wave $\pi\pi$ scattering lengths will be very difficult (see below).

Consider now the chiral expansion of the $D_{1,2}$. The LET values based on eqs.(56) are $D_1^{\text{LET}} = 2.41 \text{ fm}^3$ and $D_2^{\text{LET}} = -6.76 \text{ fm}^3$ compared to the empirical ones [18],

$$D_1^{\text{exp}} = 2.26 \pm 0.12 \text{ fm}^3 \quad D_2^{\text{exp}} = -9.05 \pm 0.36 \text{ fm}^3. \quad (69)$$

These numbers result from a best fit to the near threshold cross section data for $\pi^+ p \rightarrow \pi^+ \pi^+ n$ and $\pi^- p \rightarrow \pi^0 \pi^0 n$ [11] [15] using the correct flux and three-body phase space factors. The LET predictions show the expected pattern of deviation from the empirical values (compare the discussion in Refs.[17] [18]). The various $\mathcal{O}(M_\pi^2)$ corrections to $D_{1,2}$ are summarized in table 2.

$D_i^{(2)}$	Born	Loop	ℓ_i	c_i	GTR	N^*
1	-0.08	0.25 ± 0.13	-0.17 ± 0.18	0.24 ± 0.10	0	0
2	0.15	0.09 ± 0.48	0.39 ± 0.21	-2.85 ± 0.06	0.32	-0.40 ± 0.90

Table 2: Various M_π^2 corrections to $D_{1,2}$. All values in fm^3 .

Adding the uncertainties in quadrature, the predictions for $D_{1,2}$ to order M_π^2 are

$$D_1^{\text{thy}} = 2.65 \pm 0.24 \text{ fm}^3 \quad D_2^{\text{thy}} = -9.06 \pm 1.05 \text{ fm}^3. \quad (70)$$

These results for $D_{1,2}$ are compatible with the empirical values, eq.(69), within one standard deviation. We notice that there are large cancellations in the M_π^2 contributions to D_1 , whereas the chiral corrections to D_2 at this order are clearly dominated by the terms proportional to the low-energy constants c_i and the Roper excitation. In particular, one reads from table 2 that the loop contribution to the $I = 0$ amplitude \mathcal{A}_{10} is rather small, roughly -4% of the LET value. In contrast to this, the loop corrections for the $I = 0$ $\pi\pi$ scattering length a_0^0 are sizeable, about 25% of the current algebra value (at $\lambda = 1 \text{ GeV}$). This signals that contrary to expectations, the reaction $\pi N \rightarrow \pi\pi N$ at threshold is not very sensitive to the $\pi\pi$ final state interactions. Also, if we disentangle the terms of order $M_\pi^{(n)}$ ($n = 0, 1, 2$) we find that the convergence of the expansion for D_1 is good whereas in D_2 one still finds sizeable corrections at $n = 2$,

$$D_1 = 1.59 \cdot (1. + 0.52 + 0.15) \text{ fm}^3, \quad D_2 = -4.76 \cdot (1. + 0.42 + 0.48) \text{ fm}^3, \quad (71)$$

for the mean values of $D_{1,2}$. This shows that the chiral expansion for D_1 is converging. Matters are different for D_2 . One has at least to calculate the terms of order M_π^3 before one can draw a clear conclusion about the accuracy with which D_2 can be calculated. This, however, goes beyond the scope of the present paper.

We now turn to the determination of the S-wave $\pi\pi$ scattering lengths.^{#7} Clearly, due to the large M_π^2 corrections and uncertainties (due to the Roper) in D_2 , deducing a_0^0 from the master formula can only give an indicative result. We find

$$a_0^0 = 0.21 \pm 0.07 , \quad (72)$$

to be compared with the current algebra value of 0.16 and the CHPT prediction of 0.20 ± 0.01 [3]. We notice that the theoretical prediction has a much smaller uncertainty than the number extracted from the $\pi\pi N$ threshold amplitude.

Matters are different for a_0^2 since this quantity is entirely sensitive to D_1 . Adding the empirical and theoretical uncertainties in quadrature, we find

$$a_0^2 = -0.031 \pm 0.007 , \quad (73)$$

consistent (within one standard deviation) with the one-loop CHPT prediction of Gasser and Leutwyler, $a_0^2 = -0.042 \pm 0.008$ [2] [3]. We remark that for the combination $2a_0^0 - 5a_0^2$ we have 0.577 ± 0.144 , consistent with the universal curve, $(2a_0^0 - 5a_0^2)_{\text{univ.curve}} = 0.614 \pm 0.028$. This clearly indicates that previously determined scattering lengths based on the Olsson–Turner model [12] [16] should not be trusted. The lesson to be learned here is that even with an improved q^4 calculation there will remain sizeable theoretical uncertainties which will make a more accurate determination of the isospin zero S-wave $\pi\pi$ scattering length from the $\pi\pi N$ threshold amplitudes very difficult. In contrast, one can hope to sharpen the determination of a_0^2 , eq.(73).

7 Summary

In this paper, we have considered the reaction $\pi N \rightarrow \pi\pi N$ at threshold in the framework of heavy baryon chiral perturbation theory. The pertinent results of this investigation can be summarized as follows:

- We have calculated the chiral expansion of the threshold amplitudes D_1 and D_2 (or, equivalently, to \mathcal{A}_{10} and \mathcal{A}_{32}) up-to-and-including the quadratic order in the pion mass. This amounts to the first corrections to the low-energy theorems derived in Ref.[17]. The resulting values for $D_{1,2}$ agree with the empirical ones within one standard deviation. For D_1 , the $\mathcal{O}(M_\pi^2)$ corrections are small, the corresponding corrections to D_2 are sizeable. The latter are mostly related to chiral corrections to the πN amplitude and the excitation of the $N^*(1440)$ resonance.
- Based on this improved representation for the threshold $\pi\pi N$ amplitudes, one can deduce the isospin two S-wave $\pi\pi$ scattering length, $a_0^2 = -0.031 \pm 0.007$. This number is compatible with the one-loop chiral perturbation theory results. However, the ensuing uncertainty is still sizeable and it will be difficult to further improve

^{#7}We add the uncertainty from the theoretical determination and the one from the fit to the data in quadrature.

upon it. Due to the large M_π^2 corrections in D_2 , one can only deduce a broad range of values for a_0^0 from this calculation, $a_0^0 = 0.21 \pm 0.07$. The point here is that the threshold $\pi\pi N$ amplitudes are much less sensitive to the four-pion vertex than to other effects like resonance excitations and uncertainties in the πN amplitudes. At present, it appears that the threshold $\pi\pi N$ data are best suited to pin down the isospin two, S-wave $\pi\pi$ scattering length.

- As a by-product, we have found a new coupling for the $N^*(1440)$ decay into the nucleon and two pions in the S-wave. It differs from the conventionally used one [35] through its explicit energy-dependence (i.e. factors of the pion energies), see appendix B. It would be important to disentangle these two couplings to reduce the uncertainty related to the Roper excitation. This could eventually be done by photo-exciting the Roper and study the decay $N^* \rightarrow N(\pi\pi)_S$ in the threshold region (i.e. for $\sqrt{s} \geq m^*$).

Finally, we stress that an order q^4 calculation should be performed to further tighten the chiral predictions and to get a better handle on the chiral expansion of D_2 . Also, a consistent calculation to treat all isospin violating effects (like e.g. $m_d - m_u$, virtual photons and alike) has to be performed.

Acknowledgements

We are grateful to Jürg Gasser, Gerhard Höhler and Eulogio Oset for helpful comments. We are particularly thankful to Marc Knecht, Bashir Moussallam and Jan Stern for pointing out an inconsistency in the original version of the manuscript. We thank the Institute for Nuclear Theory at Seattle and the Svedberg Laboratory at Uppsala for hospitality extended during the completion of this work.

A Loop functions

Here, we present explicit formulae for those loop functions entering the calculation of $\pi N \rightarrow \pi\pi N$ at threshold which are not given in the review [18]. All propagators are understood to have an infinitesimal negative imaginary part in the denominator ($-i\epsilon$). We use dimensional regularization to compute divergent loop integrals and expand them around $d = 4$ space-time dimensions. In the reaction $\pi N \rightarrow \pi\pi N$ at threshold we encounter the following loop integrals involving three and four propagators,

$$\frac{1}{i} \int \frac{d^d l}{(2\pi)^d} \frac{1, l_\mu l_\nu}{v \cdot l (M_\pi^2 - l^2) (M_\pi^2 - (l + 2q)^2)} = \Phi_0(\omega), g_{\mu\nu} \Phi_3(\omega) + \dots \quad (\text{A.1})$$

$$\frac{1}{i} \int \frac{d^d l}{(2\pi)^d} \frac{1, l_\mu l_\nu}{v \cdot l v \cdot (l + 2q) (M_\pi^2 - l^2) (M_\pi^2 - (l + 2q)^2)} = \Psi_0(\omega), g_{\mu\nu} \Psi_3(\omega) + \dots \quad (\text{A.2})$$

with $\omega = v \cdot q$, $q^2 = M_\pi^2$ and the ellipsis stands for terms proportional to $v_\mu v_\nu$, $q_\mu q_\nu$, ... which are not needed in the actual calculation. For our purpose the loop functions $\Phi_{0,3}(\omega)$ defined above are to be evaluated at $\omega = \pm M_\pi + i0$,

$$\Phi_0(M_\pi) = \frac{1}{16\pi^2 M_\pi} \left[\frac{\pi}{2} - \sqrt{3} \ln(2 + \sqrt{3}) + i\pi\sqrt{3} \right] \quad (\text{A.3})$$

$$\Phi_0(-M_\pi) = \frac{1}{16\pi^2 M_\pi} \left[\frac{\pi}{2} + \sqrt{3} \ln(2 + \sqrt{3}) \right] \quad (\text{A.4})$$

$$\Phi_3(M_\pi) = 2M_\pi L + \frac{M_\pi}{16\pi^2} \left[2 \ln \frac{M_\pi}{\lambda} + \frac{\pi}{6} - \frac{5}{3} + \sqrt{3} \ln(2 + \sqrt{3}) - i\pi\sqrt{3} \right] \quad (\text{A.5})$$

$$\Phi_3(-M_\pi) = -2M_\pi L + \frac{M_\pi}{16\pi^2} \left[-2 \ln \frac{M_\pi}{\lambda} + \frac{\pi}{6} + \frac{5}{3} - \sqrt{3} \ln(2 + \sqrt{3}) \right] \quad (\text{A.6})$$

with L defined in eq.(19). In order to get the values of the functions $\Psi_{0,3}(\omega)$ at $\omega = M_\pi + i0$ one simply uses the identity

$$\frac{1}{v \cdot (l + 2q) v \cdot l} = \frac{1}{2v \cdot q} \left(\frac{1}{v \cdot l} - \frac{1}{v \cdot (l + 2q)} \right) \quad (\text{A.7})$$

shifts the loop momentum and finds

$$\Psi_0(M_\pi) = \frac{1}{2M_\pi} [\Phi_0(M_\pi) - \Phi_0(-M_\pi)] = \frac{\sqrt{3}}{32\pi^2 M_\pi^2} [i\pi - 2 \ln(2 + \sqrt{3})] \quad (\text{A.8})$$

$$\Psi_3(M_\pi) = \frac{1}{2M_\pi} [\Phi_3(M_\pi) - \Phi_3(-M_\pi)] = 2L + \frac{1}{16\pi^2} \left[2 \ln \frac{M_\pi}{\lambda} - \frac{5}{3} + \sqrt{3} \ln(2 + \sqrt{3}) - i\frac{\pi}{2}\sqrt{3} \right] \quad (\text{A.9})$$

B The decay $N^*(1440) \rightarrow N(\pi\pi)_S$

In this appendix, we discuss in detail the Roper decay into the nucleon and two pions in the S-wave since that is not treated in generality in the present literature. In fact, to order q^2 , the pertinent Lagrangian $\mathcal{L}_{N^*N\pi\pi}$ contains (at least) two terms,

$$\mathcal{L}_{N^*N\pi\pi} = c_1^* \bar{\Psi}_{N^*} \chi_+ \Psi_N - \frac{c_2^*}{m^{*2}} (D_\mu D_\nu \bar{\Psi}_{N^*}) u^\mu u^\nu \Psi_N + \text{h.c.} , \quad (\text{B.1})$$

with Ψ_{N,N^*} the relativistic spin-1/2 fields. In fact, the second term is not unique, but for the non-relativistic formulation, all relativistically inequivalent forms lead to the same operator proportional to $(v \cdot u)^2$. Using

$$\chi_+ = M_\pi^2 \left(2 - \frac{\vec{\pi}^2}{F_\pi^2} + \dots \right) , \quad u_\mu = -\frac{1}{F_\pi} \vec{\tau} \cdot \partial_\mu \vec{\pi} + \dots , \quad (\text{B.2})$$

one finds that the first (commonly used) coupling is energy-independent whereas the second depends on $\omega_1 \omega_2$, the product of the energies of the two pions. Denoting by Γ_9 the partial width $\Gamma(N^* \rightarrow N(\pi\pi)_S)$, we find using eq.(B.1),

$$\Gamma_9 = \frac{3}{16\pi^3 F_\pi^4} \int \int_{z^2 < 1} d\omega_1 d\omega_2 (m^* + m - \omega_1 - \omega_2) (c_1^* M_\pi^2 + c_2^* \omega_1 \omega_2)^2 , \quad (\text{B.3})$$

with

$$z = \frac{\omega_1 \omega_2 - m^*(\omega_1 + \omega_2) + M_\pi^2 + (m^{*2} - m^2)/2}{\sqrt{(\omega_1^2 - M_\pi^2)(\omega_2^2 - M_\pi^2)}} . \quad (\text{B.4})$$

Performing the integrals in eq.(B.3), we have

$$\Gamma_9 = \left[0.498 c_1^{*2} + 2.708 c_1^* c_2^* + 3.714 c_2^{*2} \right] 10^{-3} \text{ GeV}^3 , \quad (\text{B.5})$$

which is somewhat surprising since one would not expect the factor of pion energies leading to such a difference compared to the energy-independent coupling. Eq.(B.5) defines a rather elongated ellipse. The determination from the width does not fix the signs, we choose it to be negative for c_1^* since the first term in the Lagrangian eq.(B.1) can be considered as "transition σ -term" (analogous to the c_1 term in the dimension two pion-nucleon Lagrangian) and we know that $c_1 < 0$. Similarly, we set $c_2^* > 0$. For the threshold amplitude D_2 , only the sum of these two coupling constants is relevant. In the absence of any further empirical information, we take a mean value between the two extrema, $c_1^* = 0$ or $c_2^* = 0$, and allow for a large uncertainty to accomodate both possibilities. This leads to

$$c_1^* + c_2^* = -1.56 \pm 3.35 \text{ GeV}^{-1} , \quad (\text{B.6})$$

which we use in the main text. These two couplings could be disentangled by a precise study of the energy dependence of the Roper decay in the threshold region.

C Calculation of $D_{1,2}^{c_i}$ in the heavy mass formulation

In this appendix, we briefly sketch the derivation of the contribution $D_{1,2}^{c_i}$, eqs.(47,48), within the framework of the heavy nucleon Lagrangian. The starting point is the effective heavy nucleon action to order q^3 (for details, see appendix A of Ref.[20]),

$$S_{\pi N} = \int d^4x \bar{N} \left[\mathcal{A}^{(1)} + \mathcal{A}^{(2)} + \mathcal{A}^{(3)} + \frac{1}{2m} (\gamma_0 \mathcal{B}^{(1)\dagger} \gamma_0 \mathcal{B}^{(2)} + \text{h.c.}) + \dots \right] N , \quad (\text{C.1})$$

where the ellipsis stands for terms not contributing to the c_i/m corrections. The $\mathcal{A}^{(i)}$ and $\mathcal{B}^{(i)}$ are quantities of order q^i . While the $\mathcal{A}^{(i)}$ connect the “large” components of the heavy nucleon fields, the $\mathcal{B}^{(i)}$ give the transitions from the “large” to the “small” components before one integrates out the latter (for details, see ref.[20]). There are three different structures contributing to $D_{1,2}^{c_i}$ (from now on, we drop the superscript ‘ c_i ’). First, there are terms of the type

$$\mathcal{A}^{(2)} \frac{1}{v \cdot \ell} \frac{1}{2m} \mathcal{B}^{(1)\dagger} \gamma^0 \mathcal{B}^{(1)} , \quad (\text{C.2})$$

which lead to

$$D_1 = 2 P (-c_1 + c'_2 + c''_2 + c_3) , \quad (\text{C.3})$$

with

$$P = \frac{g_A M_\pi^2}{m F_\pi^3} . \quad (\text{C.4})$$

Second, the combination

$$\frac{1}{2m} \gamma^0 \mathcal{B}^{(1)\dagger} \gamma^0 \mathcal{B}^{(2)} + \text{h.c.} , \quad (\text{C.5})$$

contributes to D_1 and D_2 ,

$$D_1 = \frac{1}{2} P (-c'_2 + c_4) \quad D_2 = -P c_4 , \quad (\text{C.6})$$

and third, there is a D_2 contribution from

$$\mathcal{A}^{(3)} \frac{1}{v \cdot \ell} \mathcal{A}^{(1)} , \quad (\text{C.7})$$

which reads

$$D_2 = -P (c'_2 + 2c''_2) . \quad (\text{C.8})$$

Putting pieces together, we arrive at eqs.(47,48).

References

- [1] S. Weinberg, Phys. Rev. Lett. **17**, 616 (1966)
- [2] J. Gasser and H. Leutwyler, Phys. Lett. **125B**, 325 (1983).
- [3] J. Gasser and H. Leutwyler, Ann. Phys. (NY) **158**, 142 (1984).
- [4] J. Stern, H. Szadrian, and N. Fuchs, Phys. Rev. **D38**, 2195 (1988).
- [5] M. Knecht and J. Stern, Orsay preprint IPNO-TH-94-53, to be published in the second edition of the DAPHNE physics handbook, eds. L. Maiani, G. Pancheri and N. Paver.
- [6] Ulf-G. Meißner, Rep. Prog. Phys. **56**, 903 (1993).
- [7] A.A. Bolokhov, V.V. Vereshagin and S.G. Sherman, Nucl. Phys. **A530**, 660 (1991).
- [8] S. Weinberg, Phys. Rev. Lett. **18**, 188 (1967); Phys. Rev. Lett. **18**, 507 (1967); Phys. Rev. **166**, 1568 (1968).
- [9] M.G. Olsson and Leaf Turner, Phys. Rev. Lett. **20**, 1127 (1968); Phys. Rev. **181**, 2141 (1969); Phys. Rev. Lett. **38**, 296 (1977).
- [10] M.G. Olsson, Ulf-G. Meißner, N. Kaiser and V. Bernard, "On the interpretation of the $\pi N \rightarrow \pi\pi N$ data near threshold", preprint CRN 95-13, MADPH-95-866 and TK 95 07, March 1995, to appear in the πN Newsletter.
- [11] G. Kernel et al., Z. Phys. **C48**, 201 (1990); M. Sevior et al., Phys. Rev. Lett. **66**, 2569 (1991); G. Smitt et al., (CHAOS at TRIUMF, 1994). [$\pi^+ p \rightarrow \pi^+ \pi^+ n$]
- [12] D. Počanić et al., Phys. Rev. Lett. **72**, 1156 (1993); G. Smitt et al., (CHAOS at TRIUMF, 1994). [$\pi^+ p \rightarrow \pi^+ \pi^0 p$]
- [13] G. Kernel et al., Phys. Lett. **B216**, 244 (1989); G. Smitt et al., (CHAOS at TRIUMF, 1994); G. Rebka et al., (LAMPF, 1994). [$\pi^- p \rightarrow \pi^- \pi^+ n$]
- [14] G. Kernel et al., Phys. Lett. **B225**, 198 (1989); G. Smitt (CHAOS at TRIUMF), 1994). [$\pi^- p \rightarrow \pi^- \pi^0 p$]
- [15] J. Lowe et al., Phys. Rev. **C44**, 956 (1991). [$\pi^- p \rightarrow \pi^0 \pi^0 n$]
- [16] H. Burkhard and J. Lowe, Phys. Rev. Lett. **67**, 2622 (1991).
- [17] V. Bernard, N. Kaiser and Ulf-G. Meißner, Phys. Lett. **B332**, 415 (1994); (E) **B338**, 520 (1994).
- [18] V. Bernard, N. Kaiser and Ulf-G. Meißner, Int. J. Mod. Phys. **E4**, 193 (1995).

- [19] E. Jenkins and A.V. Manohar, Phys. Lett. **B255**, 558 (1991).
- [20] V. Bernard, N. Kaiser, J. Kambor and Ulf-G. Meißner, Nucl. Phys. **B388**, 315 (1992).
- [21] K.H. Watson, Phys. Rev. **95**, 228 (1954).
- [22] G. Ecker, Prog. Nucl. Part. Phys. **35**, 1 (1995).
- [23] Ulf-G. Meißner, Czech. J. Phys. **45**, 153 (1995).
- [24] G. Ecker, Phys. Lett. **B336**, 508 (1994).
- [25] V. Bernard, N. Kaiser, Ulf-G. Meißner and A. Schmidt, Nucl. Phys. **A580**, 475 (1994).
- [26] Ulf-G. Meißner, in "Chiral Dynamics: Theory and Experiment", A. Bernstein and B.R. Holstein (eds.), Springer, Heidelberg, 1995.
- [27] J. Gasser, M.E. Sainio and A. Švarc, Nucl. Phys. **B307**, 779 (1988).
- [28] J. Gasser and Ulf-G. Meißner, Phys. Lett. **B258**, 258 (1991).
- [29] A. Krause, Helv. Acta Phys. **63**, 3 (1990).
- [30] G. Höhler, in Landolt-Börnstein, vol.9b2, ed. H. Schopper, Springer, Berlin 1983.
- [31] Y. Tomozawa, Nuovo Cim. **46A**, 707 (1966).
- [32] G. Ecker, J. Gasser, A. Pich and E. de Rafael, Nucl. Phys. **B321**, 311 (1989); J.F. Donoghue, C. Ramirez and G. Valencia, Phys. Rev. **D39**, 1947 (1989).
- [33] Particle Data Group, Phys. Rev. **D50**, 1173 (1994).
- [34] G. Höhler, πN Newsletter **9**, 1 (1993).
- [35] E. Oset and M.J. Vicente-Vacas, Nucl. Phys. **A446**, 584 (1985).
- [36] J.A. Gomez Tejedor and E. Oset, Nucl. Phys. **A571**, 667 (1994).
- [37] D.M. Manley, R.A. Arndt, Y. Goradia and V.L. Teplitz, Phys. Rev. **D30**, 904 (1984).
- [38] J. Gasser, H. Leutwyler and M.E. Sainio, Phys. Lett. **B253**, 252 (1991).
- [39] J. Bijnens, G. Colangelo and J. Gasser, Nucl. Phys **B427**, 427 (1994).

Figure Captions

Fig.1 Born graphs. Solid and dashed lines denote nucleons and pions, respectively. The upper two diagrams are the contact and pion–pole graphs. The others are suppressed by powers of $1/m$ in HBCHPT.

Fig.2 Renormalization of G_π , F_π and M_π to one loop. Crosses denote counter term insertions. The double and wiggly lines represent the pseudoscalar density and the axial current, in order. For other notations, see Fig. 1.

Fig.3 Renormalization of the pion–nucleon vertex. Counter term insertions are not shown. For notations, see Fig. 1.

Fig.4 One-loop diagrams non–vanishing at threshold. Graphs with the two out–going pion lines interchanged are not shown. For notations, see Fig. 1.

Fig.5 $1/m$ suppressed contributions from the relativistic dimension two pion–nucleon Lagrangian. The circle–cross denotes an insertion from $\mathcal{L}_{\pi N}^{(2)}$ proportional to one of the low–energy constants c_i . For notations, see Fig. 1.

Fig.6 Resonance saturation. (a) and (b) refer to nucleon excitations, like the $\Delta(1232)$ or the $N^*(1440)$ (double lines) and (c) to a t–channel meson exchange (double line denoted 'R').

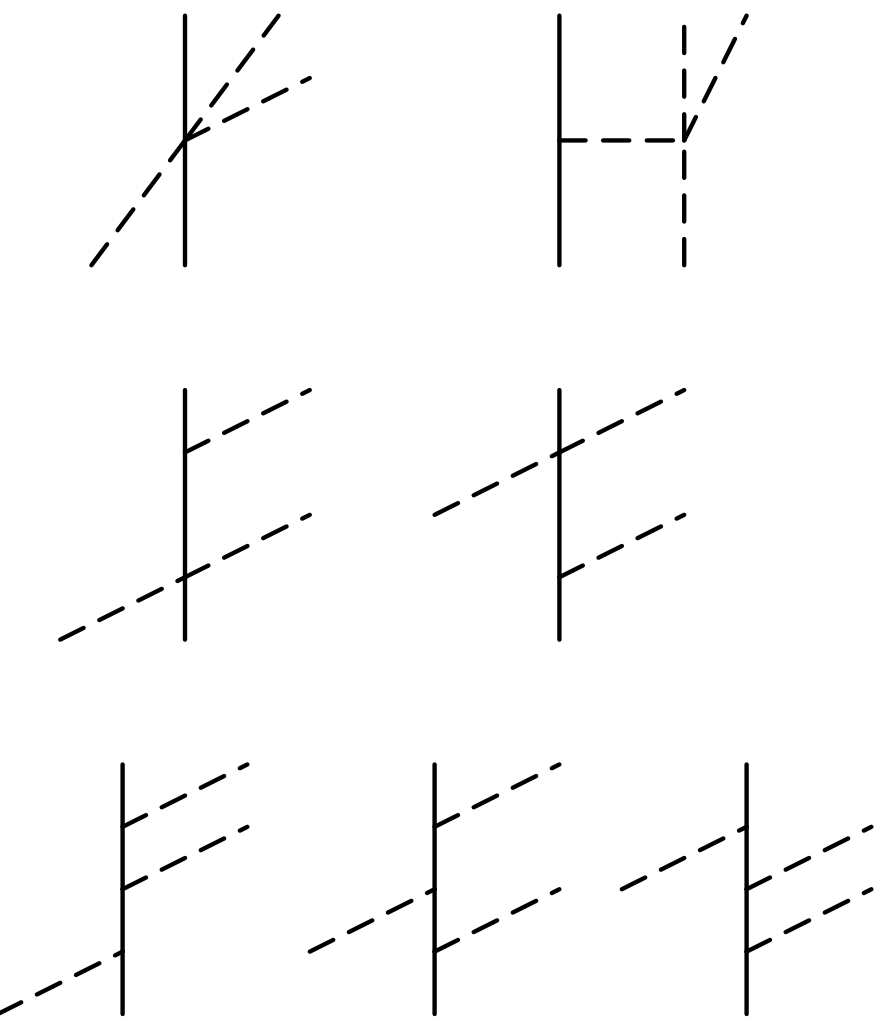


Figure 1

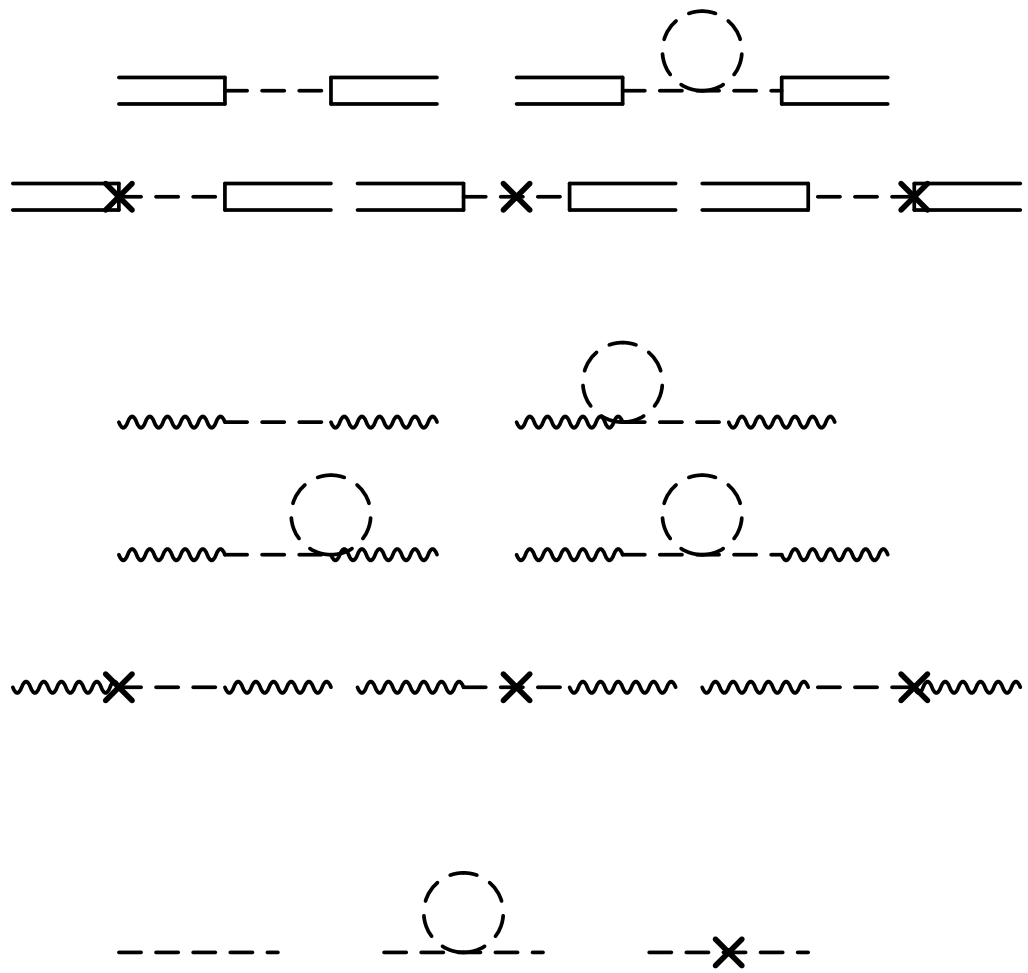


Figure 2

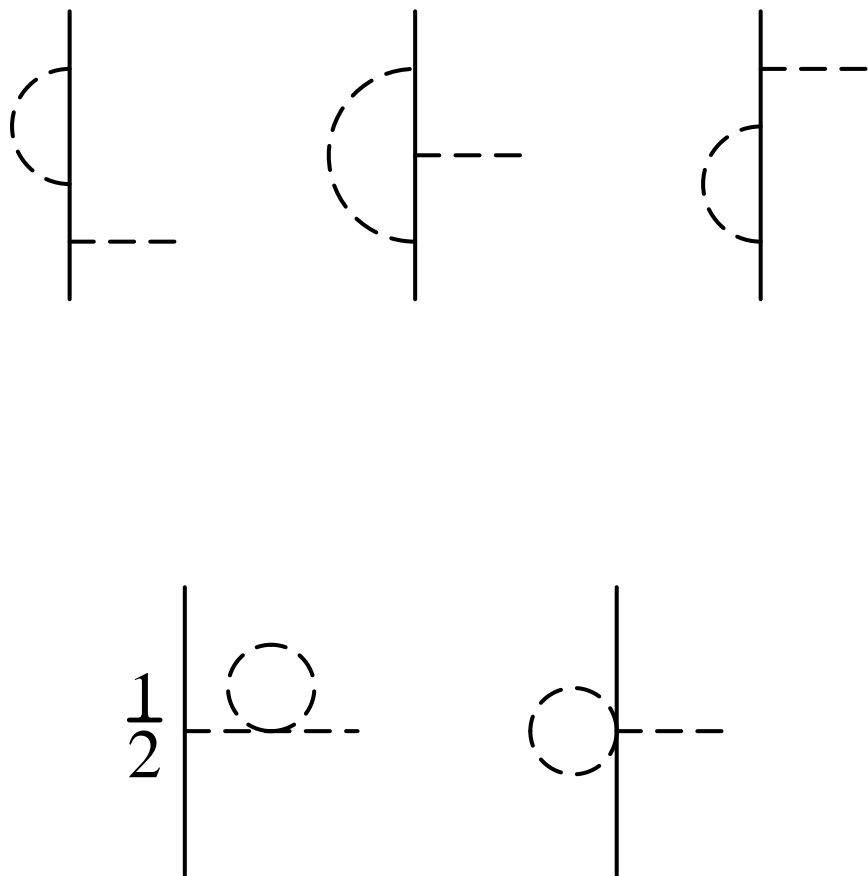


Figure 3

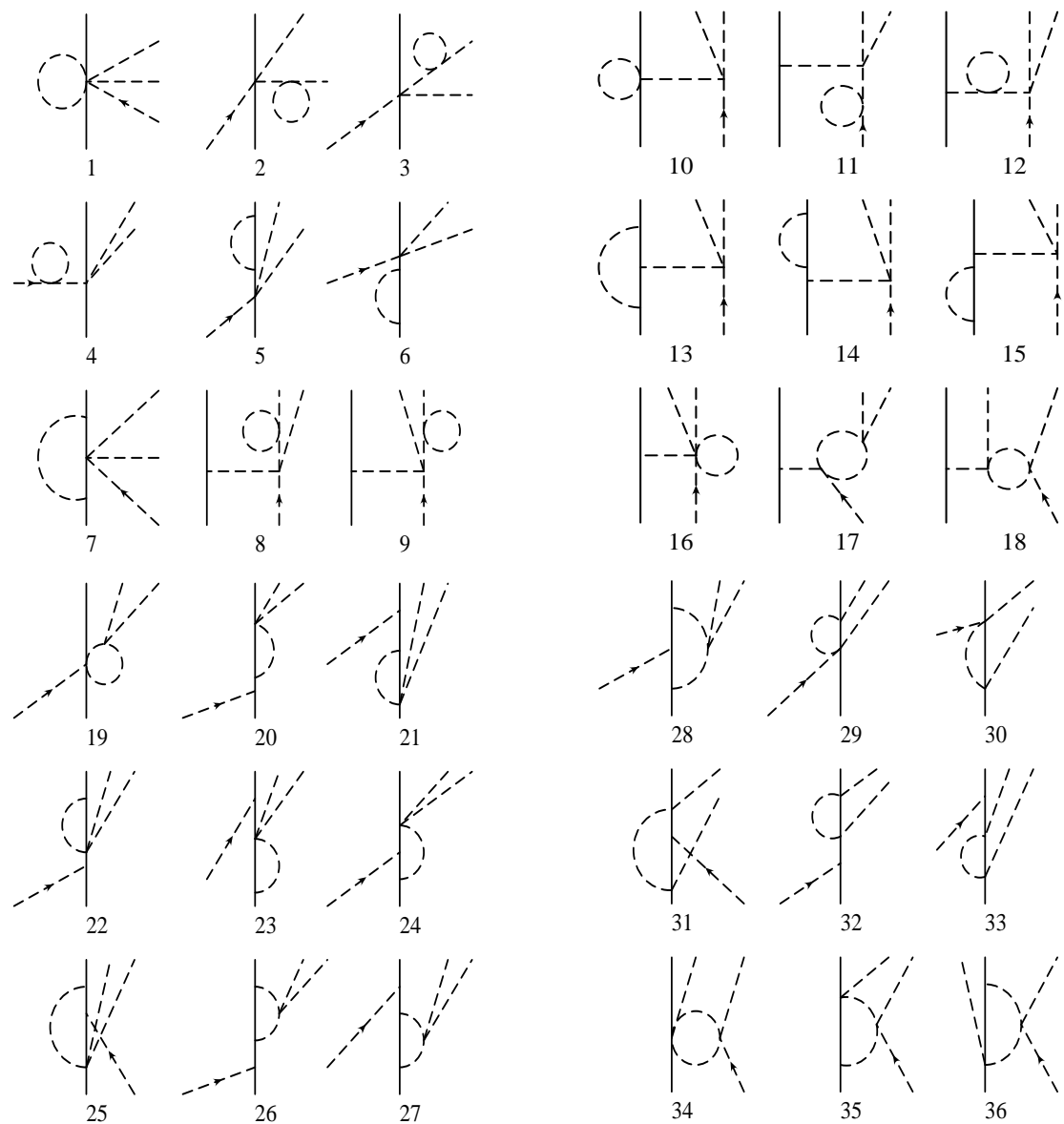


Figure 4

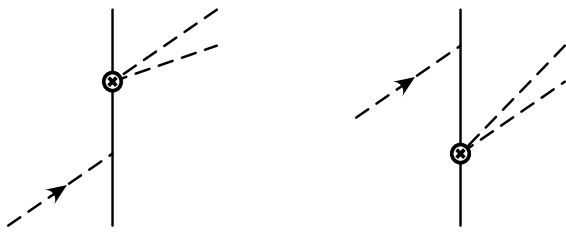
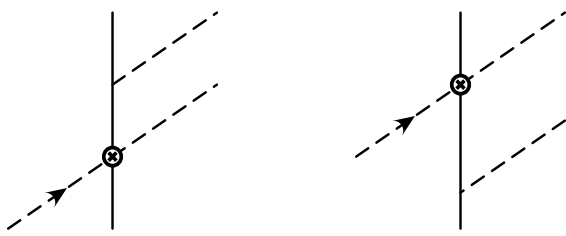
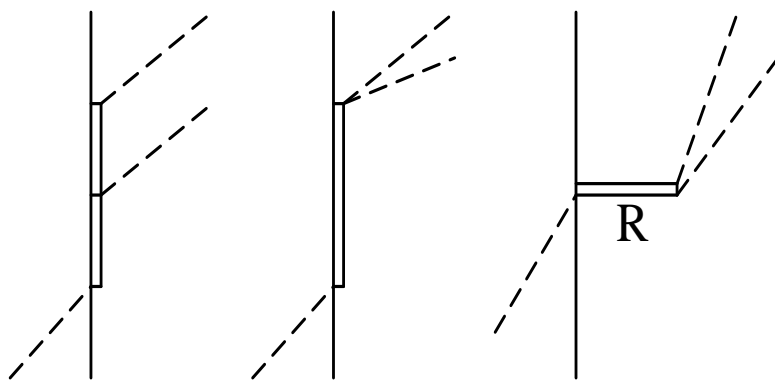


Figure 5



(a)

(b)

(c)

Figure 6